The Copernicus EMS Validation service as a vector for improving the emergency mapping based on Sentinel data

Donezar-Hoyos, U. [1]*, Albizua-Huarte, L. [1], Amezketa-Lizarraga, E. [1], Barinagarrementeria-Arrese, I. [1], Ciriza, R. [1], de Blas-Corral, T. [1], Larrañaga-Urien, A. [1], Ros-Elso, F. [1], Tamés-Noriega, A. [1], Viñuales-Lasheras, M. [1], Broglia, M. [2], Steel, A. [3], Ameztoy, I. [4], Rufolo, P. [5]

[1] Tracasa. Departamento de Ingeniería y Sistemas Territoriales. C/ Cabárceno, 6. 31621 Sarriguren. Navarra. Spain.

[2] European Commission, Joint Research Centre (JRC), Ispra. Italy.

[3] Uni Systems, Via Michelangelo Buonarroti, 39, 20145 Milan, Italy.

[4] Seidor, Via Castel Morrone, 24, 20129 Milan, Italy.

[5] Fincons group, Corso Magenta 56, 20123, Milan, Italy.

Abstract: The Copernicus Emergency Management Service (CEMS) is coordinated by the European Commission and "*provides all actors involved in the management of natural disasters, man-made emergency situations, and humanitarian crises with timely and accurate geo-spatial information derived from satellite remote sensing and complemented by available in situ or open data sources*". It includes two components, Early Warning and Monitoring and Mapping. The latter provides on demand geo-spatial information derived from satellite imagery during all phases of the disaster management cycle. It includes 3 systems, Rapid Mapping (RM), Risk and Recovery Mapping (RRM), and a Validation Service. RM provides geospatial information immediately after a disaster to assess its impact; RRM in the prevention, preparation and reconstruction phases; and the Validation Service is in charge of validating and verifying the products generated by both, and of collecting and analyzing users' feedback. The wide spectrum of activities framed in the Validation Service has allowed it to become a vector to improve the Mapping component through the testing of new methodologies, data input type, or approach for the creation of emergency cartography in the frame of the CEMS. The present paper introduces the main investigation lines based on Sentinel-1 and 2 for flood and fire monitoring that could be implemented in the CEMS services taking into consideration the characteristics of the Mapping component in terms of products to create and time constraints. The applicability of Sentinel-1 for flood monitoring based on the backscattering, the MultiTemporal Coherence (MTC), and dual polarization; and for burnt area delineation based on MTC was studied, while Sentinel-2 was used for burnt area delineation based on vegetation indices. Results indicate that proposed methodologies might be appropriate for the creation of crisis information products in large areas, due to the relative easy and fast implementation compared to classic photo interpretation, although further applicability analyses should be carried out.

Key words: Copernicus, Emergencies, CEMS, Validation, Sentinel-1, Sentinel-2, mapping, flood, fire.

El Servicio de Validación de Copernicus EMS como vector de mejora de la cartografía de emergencias basada en Sentinel

Resumen: El Servicio de Gestión de Emergencias de Copernicus (CEMS), está coordinado por la Comisión Europea y "*provee de información geoespacial precisa y oportuna derivada de la teledetección satelital y completada por fuentes de datos disponibles in situ o abiertas a todos los actores involucrados en la gestión de emergencias, bien sean derivadas de desastres naturales o producidos por el hombre, o de crisis humanitarias*". El servicio tiene dos componentes, uno de alerta temprana y monitoreo y otro de creación de mapas. El servicio de mapeo se encarga de proveer, bajo demanda, a los diferentes agentes de emergencias de información geoespacial derivada de imágenes de satélite en todas las fases de la gestión de emergencias, consta de 3 sistemas, *Rapid Mapping* (RM), *Risk and Recovery Mapping* (RRM), y *Validation*. RM aporta información inmediatamente después de un desastre para evaluar su impacto; RRM en las fases de prevención, preparación y reconstrucción; y la Validación se encarga de validar y verificar los productos generados por ambos, y de recoger y analizar los comentarios de los usuarios. El amplio espectro de actividades enmarcadas en él le ha permitido ser vector de mejora de los servicios de mapeo de emergencias mediante el testeo de nuevas metodologías, tipos de datos, o enfoques para la creación de cartografías de emergencias en el marco de CEMS. El presente artículo describe las principales líneas de investigación en el uso de datos Sentinel-1 y 2 para la monitorización de inundaciones e incendios, que se podrían implementar en el futuro en el marco de CEMS. La aplicabilidad de Sentinel-1 para el monitoreo de inundaciones basado en la retrodispersión, la coherencia multitemporal (MTC) y la polarización dual; y se estudió la delimitación del área quemada basada en MTC. Sentinel-2 se usó para delimitar áreas quemadas en base a índices de vegetación. Los resultados indican que las metodologías propuestas podrían ser apropiadas para la creación de productos de información de crisis en grandes áreas, debido a la implementación relativamente fácil y rápida en comparación con la fotointerpretación clásica, aunque deberían realizarse más análisis para su aplicación en el marco de CEMS.

Palabras clave: Copernicus, Emergencias, CEMS, validación, Sentinel-1, Sentinel-2, cartografía, inundación, incendio.

1. Introduction

Copernicus is the European Programme for the establishment of a European capacity for Earth Observation. The Copernicus Emergency Management Service, CEMS, coordinated by the European Commission, "*provides maps and analyses based mainly on satellite imagery (before, during or after a crisis) as well as early warning services for flood, fire, and drought risks. Through these services, it supports crisis managers, Civil Protection authorities and humanitarian aid actors dealing with natural disasters, man-made emergency situations, and humanitarian crises, as well as those involved in disaster risk reduction, preparedness and recovery activities*" (CEMS, 2020). The service is comprised by Early Warning and Monitoring, and Mapping components.

The Early Warning and Monitoring component includes three systems, the European Flood Awareness System (EFAS), the European Forest Fire Information System (EFFIS) and the European Drought Observatory (EDO), which provide information on forecasting and monitoring of floods in Europe, and on forest fires and drought and its ecological impact in Europe, Middle East and North of Africa. EFAS is the only system with restricted access for real-time forecast and products, while the two others have viewers from which the information can be consulted and downloaded (CEMS, 2017).

The CEMS Mapping component, operational since April 2012, is an on-demand service that can be activated by an Authorised User included in the following categories (1) National Focal Points, (NFP), *i.e.*, Civil Protection authorities of the Member States; (2) European Union services such as Directorate General for the European Commission Humanitarian Aid & Civil Protection (DG ECHO), and (3) The European External Action Service (EEAS). At the DG ECHO, the Emergency Response Coordination Centre (ERCC) acts as the contact point for international governmental and non-governmental. The service can be activated in two modes, Rapid Mapping (RM) for the creation of maps and crisis-related information immediately after the disaster event, and Risk and Recovery

Mapping (RRM) for the creation of reference and/or crisis information usable in the prevention, readiness and reconstruction phases after a disaster or emergency event. Every request, if approved by the ERCC, results into an activation in the frame of which mainly satellite images are acquired to create crisis information of different nature within the Areas of Interest (AOI) defined by users. The Mapping component includes the Copernicus EMS – Mapping Validation Service used for the verification of a sample of service outputs produced by RM and RRM services, carried out independently from them, and triggered by the European Commission. The validation methodology is based on the validation protocol developed by the Joint Research Centre (JRC) (Broglia et al., 2010), mainly focused on geometric and thematic accuracy assessment. This document is the basis for the validation procedures that are carried out in the frame of the Validation Service.

The Validation Service tests data and methods that could be used to create the CEMS products in the frame of the continuous improvement of the service and gathers the opinions and feedback of users to spot improvement topics (CEMS, 2018). Its activities have extended from the mere thematic accuracy assessment of the Mapping component products to the research of alternative methods and input data that could be used to create the crisis information. Results created in the scope of the Validation Service are not public, and are only distributed to Authorised Users and Mapping Service Providers.

Given that the deployment of the Sentinel satellites has gone in parallel to the evolution of the validation service, special emphasis has been put in exploring the use of the free information they provide to create crisis information. The present paper aims at introducing the main investigation lines, within the CEMS Validation Service, based on Sentinel-1 and 2 for flood and fire monitoring, and the main results of these investigations, based on which, a summary of recommendations were made to the CEMS along the years. The final goal is the implementation of data sources and alternative methods to those already in use in CEMS that could be used onwards, taking into consideration the characteristics of the Service in terms of time constraints and type of data to be created.

2. Materials and methods

The main lines of research using Sentinel-1 and 2 data in the frame of the CEMS for flood and fire monitoring are presented in the following subsections. They correspond to studies where Sentinel-based crisis data were derived (1) to use as reference data to validate specific CEMS products, or (2) to be compared/validated against reference data. These studies were located in different areas of the world. In all cases, reference data correspond to data created using images of higher spatial resolution, and/or optical in the case of the information derived from Sentinel-1. Table 1 summarizes the research lines and the study cases considered for this paper, along with their location.

Table 1. Summary of lines of research and application of Sentinel data. S1 stands for Sentinel-1 and S2 stands for Sentinel-2.

Application	Method	Validation case	Study area*
Sentinel-1 for flood delineation	Analysis of backscatter	(Case 1) S1-derived flood layer *vs.* COSMOSkyMed-derived flood layer	USA
	MTC	(Case 2) S1-InSAR-derived flood layer *vs.* Rapid-Eye- derived flood layer	Perú
		(Case 3) S1-InSAR-derived flood layer *vs.* S1 backscatter derived flood layer (23/03/2017)	
		(Case 4) S1-InSAR-derived flood layer *vs.* S1 backscatter derived flood layer (27/03/2017)	
	VV-VH dual polarization	(Case 5) Qualitative analysis	USA
Sentinel-2 for fire delineation	dNBR, dBAI calculation	(Case 6) S2-derived fire layer *vs.* Photo interpretation of Worldview (pre-event) and SPOT (post-event)	Greece
Sentinel-1 for fire delineation	MTC	(Case 7) S1-InSAR- derived fire layer *vs.* S2-derived fire layer	

* Due to service restrictions, no details regarding the study areas can be published.

Some of the decisions taken in the creation of the Sentinel-based crisis information shall therefore be seen in the light of this frame, such as the choice of different Minimum Mapping Units (MMU), which took into consideration the scale of the product under validation based on the works of Lencinas and Siebert (2009), Priego et al. (2010), and on our expertise. In this document t1 and t2 stands for the pre- and the post-event dates.

2.1. Sentinel data applied to flood monitoring

Sentinel-1 holds a C-band instrument that can operate in single (HH or VV) and dual polarization (HH+HV and VV+VH) (ESA, a). Nevertheless, the primary conflict-free modes are IW, with VV+VH polarisation over land. Its usability for flood delineation and monitoring was tested in different areas following three different approaches.

2.1.1. Flood delineation based on the analysis of backscatter

The first approach was based on the classification of the backscatter coefficient of Sentinel-1 images considering the low backscatter values of water due to specular reflection of the transmitted beam over smooth surfaces (Shen et al., 2019), which has been widely tested in the past. The aim was to test the possibility to discriminate water despite the fact that other studies indicate that the HH polarization, of which Sentinel-1 mostly lacks and was not available in the cases here presented, is the most appropriate to discriminate water (Henry et al., 2006). The case presented here was chosen because, in a specific RM activation, the Sentinel-1 flooded area delineation was carried within a large AOI, $23\,000$ km², and the derived delineation was compared to the delineation in the RM product, produced over a COSMO-SkyMed image for which the HH polarization was available, see Table 1. Sentinel-1 image was Ground Range Detected (GRD) acquired. Even if dual polarization was available, only VH was processed, based on the worse results using VV of previous experiences and available scientific literature (Henry et al., 2006). Information derived from VH polarization of Sentinel-1 image was compared to information derived from HH of COSMO-SkyMed image. A Sentinel-2 image displayed in natural colour was used as a pre-event image.

The Sentinel-1 image was radiometrically calibrated and geometrically corrected and the resulting backscatter image was classified following an object-based approach, setting a MMU of $10\,000$ m², for flood delineation.

2.1.2. Flood delineation based on the analysis of MultiTemporal Coherence

The second approach studied the feasibility to monitor the flooded area from the analysis of the Interferometric Synthetic Aperture Radar (InSAR) coherence in a wide area that remained flooded for more than two months due to massive flooding. For each analysed date within that period, the MultiTemporal Coherence (MTC) image, a stack of three bands, which depicts the t1 and t2 intensity in the Red and Green bands respectively, and the t1-t2 coherence in the Blue, was calculated and classified. The local coherence, *i.e.*, coherence at a given point, is the cross-correlation coefficient of a SAR image pair estimated over a small window, a few pixels in Range x Azimuth (Ferretti et al., 2017a). The coherence image is obtained computing the absolute value of the local coherence on a moving window that covers the whole SAR image. The images shown in Table 2 were used in the study.

Table 2. Imagery used in the study of the applicability of MTC to flood monitoring.

Sensor	Date	Polarisation	Pass
Sentinel-1	11/03/2017	VV-VH	Ascending
	23/03/2017		
	20/03/2017	VV	Descending
Sentinel-1	26/03/2017		
Sentinel-1	01/04/2017	VV-VH	

All images were Single Look Complex (SLC) products, acquired in the interferometric wide swath (IW) mode, which maintain the phase information, necessary to calculate coherence. The pixel spacing for these products is 2.3×14.1 m in Range×Azimuth (ESA a). No multi-looking was applied in order not to decrease the spatial resolution of the input images (ESA b), but a speckle filter was used to decrease noise. Coherence was calculated for each monitoring date with the t1-t2 image pairs shown in Table 3.

The generation of the flooded area for each of the monitoring dates followed the workflow shown in Figure 1. Water extent was obtained over the

MTC images for each day by an object-based classification of these images. Flooded area was then obtained by removing from the water extent the permanent water on the Water Occurrence (1984-2015) data (Pekel et al., 2016) from the Global Surface Water, considering as permanent water those pixels with a water probability value above 40%.

Table 3. Image pairs considered for the calculation of coherence for each monitoring date.

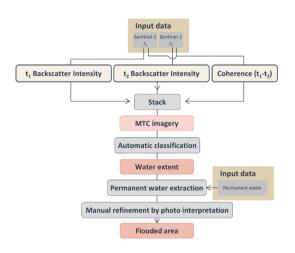| Monitoring date	t1	t2
23/03/2017	11/03/2017	23/03/2017
26/03/2017	20/03/2017	26/03/2017
01/04/2017	26/03/2017	01/04/2017

Figure 1. General workflow for the extraction of flooded area based on MTC images.

Data created with this methodology was validated against flooded area data derived by the classification of backscatter of Sentinel-1 images of the 23/03/2017 and 26/03/2017 and a RapidEye image of 01/04/2017. All these layers were obtained using a semi-automatic approach, with an automatic classification followed by minor editing by photo interpretation, and using a MMU of 625 m^2.

2.1.3. Flood delineation based on VV-VH dual polarisation

The third approach implemented a method proposed by Jo et al. (2018) that takes advantage of pre- and post-event Sentinel-1 images and their dual polarisation VV-VH to derive flood, aiming to overcome the lack of HH polarisation in Sentinel-1 while profiting from the short revisit time of Sentinel-1 (ESA, a) that makes possible to have pre- and post-event images acquired in a short period of time. Table 4 shows the input Sentinel-1 data used in the study. No reference data was available for this approach and therefore only a visual qualitative assessment of the results was carried out.

Table 4. Sentinel-1 images used in the analysis of flooded areas based on Jo et al. (2018).

Sensor	Date	Polarisation
Sentinel-1	24/08/2017 (pre-event)	VV-VH
	30/08/2017 (post-event)	

The workflow for the processing is shown in Figure 2. The RGB false-colour composite in decibels (dB) scale was generated, and used as input in the classification for flood delineation. A MMU of 1000 m^2 was established.
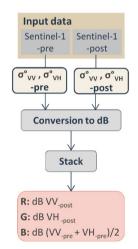

Figure 2. Workflow for the generation of RGB composite to extract the flooded area based on pre- and post-event Sentinel-1 images.

2.2. Sentinel data applied to burnt area delineation

Having fast methods for accurate delineation of burnt areas is key for an efficient and fast response. In the scope of the CEMS Validation service two approaches have been investigated using Sentinel data for burnt areas delineation, based on vegetation indices calculated using Sentinel-2 and on MTC calculation using Sentinel-1 data.

2.2.1. Burnt area delineation based on Sentinel-2 data

The temporal and spectral range of Sentinel-2 imagery are the two main advantages of this sensor to delineate and monitor burnt areas (ESA, c). The former allows having images every 5 days at the equator or about 3 days at mid latitudes, and therefore the calculation of differential indices that consider the situation before and after the event, decreasing the chances of having false positives. The latter allows the calculation of the Normalised Burnt Ratio (NBR) over the Near InfraRed (NIR) and the Short Wave InfraRed (SWIR) bands (Cocke et al., 2005). Two vegetation indices were calculated for each date, the NBR and the Burnt Area Index (BAI) (Fornacca et al., 2018).

$$NBR = (NIR - SWIR) / (NIR + SWIR) \qquad (1)$$

and

$$BAI = 1/((0.1 - Red)^2 + (0.06 - NIR)^2) \qquad (2)$$

Where Red = Band 4; NIR = Band 8 and SWIR = Band 12 of Sentinel-2 (ESA, c).

The following table summarises the images used in the comparison.

Bands 4 and 8 are acquired at a spatial resolution of 10 m, while band 12 is acquired at 20 m. Aiming to overcome the limitation that the difference in spatial resolution entailed creation of the burnt area delineation at the highest possible spatial resolution, the band at 20 m was super-resolved to 10 m in SNAP using the Sen2Res tool (ESA, d). This approach allowed calculation of the vegetation indices at 10 m.

Burnt area delineation based on Sentinel-2 was derived by an object-based classification considering a MMU of 900 m², *i.e.* 9 pixels. Different tests were carried out to investigate which vegetation index was more suitable for burnt area delineation, considering that the characteristics of the terrain, *i.e.* mountainous with scarce Mediterranean vegetation made identification of burnt areas difficult. Best results were obtained classifying a combination of both vegetation indices.

Reference data used for comparison in this analysis was created by photo interpretation of pre- and post-event Very High Resolution (VHR) optical images, WorldView images for the pre-event and a SPOT 7 images for the post-event.

2.2.2. Burnt area delineation based on Sentinel-1

To overcome the limitations of optical imagery due to cloud or smoke cover, or their acquisition being restricted to daylight hours, several studies such as the one carried out by Tanase et al. (2011) have analysed SAR data to delineate burnt areas, mainly focused on the analysis of the differences between the pre- and post-fire situations, using both the backscatter and the coherence data. The MTC analysis used in this approach as an alternative to optical-based indices for mapping forest fires has not been widely tested yet. A complete description of the analysis carried out was already presented in Donezar et al. (2019), including the study of the most appropriate polarization or the combination of images acquired in Ascending or Descending modes that might compensate the effect of the topography in the images. Being this paper a compilation of several studies, only the approach that gave better results in the thematic validation are included here. Best results were obtained when MTC images derived from Ascending and Descending images in VH polarization were combined.

In this study, 4 Sentinel-1 images were processed to obtain the burnt area delineation and tested against reference data derived from Sentinel-2 images. All Sentinel-1 images were acquired

Table 5. Imagery used in the study of Sentinel-2 applied to burnt area delineation.

Sensor	Time	Date	GSD*	Acquisition Mode	Off-nadir angle**	Cloud coverage
Sentinel-2	t1	09/08/2019	10 m	Level 2A	NA	0%
	t2	24/08/2019				
WorldView-2	t1	27/04/2019	0.5 m	-	14.4°	
WorldView-3				-	27.9°	
SPOT 7	T2	24/08/2019	1.5	-	25.7°	

* Ground Sample Distance.
** Although S-2 images show different angles along their swath, it is usually considered that the angle is 0˚ on average.

Table 6. Imagery used in the study of Sentinel-1 applied to burnt area delineation.

Sensor	Time	Date	GSD*	Acquisition Mode	Pass	Polarization	Angle**
Sentinel-1	t1	02/09/2016	14 m	Interferometric Wide	Ascending	VV, VH	30.6° to 41.6°
	t2	14/09/2016		Swath (IW)			
	t1	08/09/2016			Descending		41.5° to 45.9°
	t2	20/09/2016					
Sentinel-2	t1	19/08/2016	10 m		-	-	0°
	t2	18/09/2016		Level 1C	-	-	
SPOT 6	t2	15/09/2016	1.5 m	-	-	-	20°

* Ground Sample Distance.
** Although S-2 images show different angles along their swath, it is usually considered that the angle is 0˚ on average.

with double polarization as SLC products. The pixel spacing for these products is 2.3×14.1 m in Range×Azimuth (ESA, a). No multi-looking was applied in order not to decrease the spatial resolution of the input images. Sentinel-2 images were acquired as Level 1C, *i.e.*, without atmospheric correction, as Level 2A products were not available at the time. Table 6 summarizes the imagery used.

The processing of Sentinel-1 images until the calculation of the MTC image followed the workflow in Figure 1. Burnt area delineation based on Sentinel-1 data was carried out by classification of the MTC image with a fixed MMU of 1500 m^2.

2.3. Processing environment

All the processing carried out to Sentinel data in the scope of the studies presented in this document was done entirely in SNAP unless otherwise specified. The Shuttle Radar Topography Mission (SRTM) of 1 or 3 arcsec provided by the USGS (US Geological Survey, N.d.) was used as source of elevation information.

The calculation of coherence was carried out in SNAP using the default values of the moving window, as past experiences (Donezar et al., 2017) showed that those values, 10×2 m coherence Range×Azimuth window size, are appropriate and results are optimal for Sentinel-1. Coherence pixel values range from 0 to 1, where 1 is total coherence between images and 0 is no coherence. Excluding random noise, the coherence is determined by the changes with time of the scattering properties of a target (Ferretti et al., 2017b).

In all cases, delineation of crisis information was based on object-based classifications using Feature Analyst™ of images resulting from processing carried out in SNAP software (Textron Systems) running in an ESRI environment, that uses a hierarchical learning process to segment the image based on categories determined by the user.

2.4. Accuracy measurements for validation of crisis data

Validation was carried out following an area-based approach and the template shown in Table 7. Accuracy measurements include OA (%), *i.e.*,

Table 7. Validation template used in the validation of Sentinel-based crisis information.

		Reference Data				
		Crisis (c)	No crisis (n)	TOTAL	User's Acc. (%)	Commission error (%)
Sentinel based data	Crisis (c)	n_{cc}	n_{cn}	$n_{cc}+n_{cn}$	$(n_{cc}/(n_{cc}+n_{cn}))\times100$	$(n_{cn}/(n_{cc}+n_{cn}))\times100$
	No crisis (n)	n_{nc}	n_{nn}	$n_{nc}+n_{nn}$	$(n_{nn}/(n_{nc}+n_{nn}))\times100$	$(n_{nc}/(n_{nc}+n_{nn}))\times100$
	TOTAL	$n_{cc}+n_{nc}$				
	Producer's acc. %	$(n_{cc}/(n_{cc}+n_{nc}))*100$				
	Omission error %	$(n_{nc}/(n_{cc}+n_{nc}))*100$				
					OA%	$((n_{cc}+n_{nn})/N)\times100$
					OAu%	$(n_{cc}/(n_{nc}+n_{cc}+n_{cn}))\times100$
					Cu%	$(n_{cn}/(n_{nc}+n_{cc}+n_{cn}))\times100$
					Ou%	$(n_{nc}/(n_{nc}+n_{cc}+n_{cn}))\times100$

the overall accuracy taking the whole AOI into consideration, and OAu (%), Cu (%) and Ou (%), which correspond to the overall accuracy, commission and omission errors respectively, taking into consideration the union of the crisis information in both layers under comparison.

3. Results

The following table includes the OA (%), OAu (%), Cu (%) and Ou (%) for every validation case presented in the document.

In validation *Case 1*, a flooded area product created with a COSMO-SkyMed of 30 m was validated against the flooded area derived from Sentinel-1 backscatter analysis. Discrepancies were mainly due to (1) the lower pixel spacing of COSMO-SkyMed acquired at 30 m compared to the one of Sentinel-1, 10 m (ESA, b), (2) the criteria followed to extract the flooded area and (3) the differences in the polarisation and bands of the images used as input data, VH and C-band for Sentinel-1 and HH and X-band for COSMO-SkyMed. Even if the polarization of COSMO-SkyMed was *a priori* considered more suitable, the results shows that VH worked well. More errors of omission than of commission were encountered, meaning that the classification based on COSMO-SkyMed underestimated the flooded area. Results were checked with available optical imagery that confirmed that the classification of Sentinel-1 was correct.

Results of the application of MTC methodology for flooded area delineation in *Cases 2 to 4* showed similar results in the comparison against RapidEye or against the Sentinel-1 backscatter based classifications, with most discrepancies located in shallow water areas or in areas where water carried large quantities of sediments. High overall accuracy values for the union of the crisis information point to a promising approach.

No reference data was available for *Case 5*, and therefore a visual analysis of results was carried out. Most misclassifications were located in urban areas, due to intrinsic radar limitations. However, the analysis of the false colour composite using dual polarisation VV-VH of Sentinel-1 and pre- and post-event images as RGB components allowed to distinguish between existing standing water in the pre-event and recently flooded areas.

High overall accuracy values for the union of the crisis information were observed in validation *Case 6* (88%) together with omission and commission values for the union below 10%. It should be outlined that the study was carried out in a steep terrain with scarce vegetation where the photointerpretation of the burnt area was very difficult. To this difficulty, the difference in the appearance of the pre-and post-imagery used to create the reference data due to their acquisition time was added. Pre-event VHR optical imagery was acquired in April, and vegetation appeared vigorous, while

Table 8. Results of thematic validation for each case. Numbering of cases are included as in Table 1.

Application	Validation case	OA(%)	OAu(%)	Cu(%)	Ou(%)
Sentinel-1 for flood delineation	(Case 1) COSMO-SkyMed-derived flood layer *vs.* S1-derived flood layer*	98	50	19	31
	(Case 2) S1-InSAR-derived flood layer *vs.* Rapid-Eye- derived flood layer	88	65	1	35
	(Case 3) S1-InSAR-derived flood layer *vs.* S1 backscatter derived flood layer (23/03/2017)	91	77	10	14
	(Case 4) S1-InSAR-derived flood layer *vs.* S1 backscatter derived flood layer (26/03/2017)	95	76	4	21
	(Case 5) Qualitative analysis	-	-	-	-
Sentinel-2 for fire delineation	(Case 6) S2-derived fire layer *vs.* Photo interpreteion of Worldview (pre-event) and SPOT (post-event)	94	88	7	5
Sentinel-1 for fire delineation	(Case 7) S1-derived fire layer *vs.* S2-derived fire layer	97	66	15	19

* In this case, as the Sentinel-1 data was considered a better source of data, the Sentinel-1 based crisis information was taken as reference in the validation.

the fire took place in August, where the senescent vegetation looked similar to the burnt vegetation.

An area with similar characteristics was studied in *Case 7*, *i.e.* mountainous with scarce Mediterranean vegetation. Results showed high overall accuracy values for the union of the crisis information, 66%, and low omission and commission values for the union of the crisis information. This approach had already been tested in an area with different characteristics, flat with a dense forest and agricultural plots (Donezar et al., 2017), where results for the overall accuracy, commission and omission of the union of the crisis information were 66%, 4% and 30%, respectively. High omission values were due to the presence of agricultural plots that in the moment the fire took place had no vegetation and were not classified as burnt in the Sentinel-1 based classification. In the present case, most discrepancies were caused by the shadows due to the steep terrain.

4. Discussion and conclusions

The results seem to indicate alternative input data and methodologies that might be appropriate for the creation of crisis information products in large areas, due to the relative easy and fast implementation when compared to classic photointerpretation, although further applicability analyses should be carried out for their application in the frame of CEMS. The methods described here are being already implemented in the CEMS Validation Service.

Taking into account that some of the events are characterised by adverse visibility conditions such as high cloud coverage or the presence of smoke or haze, the applicability of Sentinel-1 data is of special interest. However, the intrinsic limitations of radar in forest and urban areas should be taken into consideration and potential users shall be informed about them in order to ensure that crisis information products are not misinterpreted.

Despite the good results that the MTC approach has shown in the different applications tested, it should be taken into consideration that coherence, which is defined as the cross-correlation product derived from two co-registered complex-valued SAR images, (Lu and Zhang, 2014) depicts the similarity of the radar reflection between them. Any changes in the complex reflectivity function

of the scene are manifested as a decorrelation in the phase of the pixels between two images, (Closson and Milisavljevic, 2017) resulting in a loss of coherence. Therefore, the use of MTC in disaster mapping assumes that the loss of coherence is due to the event itself, that no other sources of decorrelation are present. The return period of Sentinel-1, that allows to calculate coherence with images acquired in a time gap of 6 days (ESA, a), gives ground for making the assumption that changes are due to the considered event.

Despite the positive results shown, the pixel size of the Sentinel images negatively affects the accuracy and the precision of the resulting thematic layer, and has therefore a direct impact on the working scale that can be considered. With regards to the creation of fire delineation products in the scope of CEMS Rapid Mapping service, limitations caused by the spatial resolution of HR Sentinel-1 and 2 sensors, compared to the spatial resolution of VHR sensors should be considered. These VHR data, usually preferred by the users in order to create the crisis information in the CEMS products, are derived from sensors included in the Copernicus Contributing Mission Entities (CCME 2020), which are available to the service through the Copernicus Space Component Data Access (CSCDA)-ESA mechanism (Copernicus Space Component Data Access).

4.1. Flood delineation based on the analysis of backscatter

In the testing of Sentinel-1 of 10m to create flooded delineation over wide areas compared to the information created over a COSMO-SkyMed of 30 m, results showed that despite not having the HH polarization, the information created over Sentinel-1 had higher accuracy. These results highlight the importance of the spatial resolution and the classification criteria to appropriately delineate flood. The difference in the bands used by both sensor, C in the case of Sentinel-1 and X in COSMO-SkyMed, might also partly explain the differences, as X-band is more sensitive to terrain roughness (ESA, e).

Moreover, the test showed the capabilities of Sentinel-1 in the creation of crisis information in wide areas with a single image. It was noticed that in the product the criteria to classify flood varied

within the AOI, and areas with similar response in the post-event image were classified as *Flooded* or *Not flooded* indistinctly. A possible reason for this might be that the size of the AOI, more than 23 000 km², made more difficult to create uniform data. This highlights the importance of having a classification methodology that might be used efficiently in wide areas while obtaining a trade-off between the omissions and commissions.

4.2. Flood delineation based on the analysis of MultiTemporal Coherence

Results of the validation showed that flood delineation based on MTC could adequately reflect the evolution of deep-flooded areas, even if it shows a decrease in the performance of water detection in areas with shallow waters or with a high concentration of sediments. Over the years it has been observed that the performance of Sentinel-1 in such areas is worse than in deep-flooded areas, also when using the backscatter as source of information.

4.3. Flood delineation based on VV-VH dual polarisation

The analysis of the false colour composite using VV-VH polarisation of Sentinel-1 allowed to distinguish between existing standing water in the pre-event image and flooded areas. This method of flood mapping allows to rapidly derive flooded areas, which is important in an emergency context, and does not depend on the availability of permanent water information. This approach is promising as the high revisit time of Sentinel-1 would allow its implementation in almost any cases.

4.4. Burnt area delineation based on Sentinel-2

The effect of the algorithm in SNAP to super-resolve the Sentinel-2 bands, Sen2Res, was analysed by comparing the statistics of the resulting image with those of the original image and with those obtained by carrying out a mere resampling, showing only minor changes. However, other available algorithms that have given more consistent results in the calculation of super-resolved bands such

as DSen2 could be explored. Results of the calculation of vegetation indices over super-resolved images to be used as a reliable source for the creation of crisis information are promising.

Results seem to indicate that in certain cases such as the one studied where available pre- and post-event VHR optical images have high acquisition angles or a very different appearance that hinders photo interpretation, Sentinel-2 could be prioritised for burnt area delineation. Despite the limitations due to its lower spatial resolution, its higher revisit time and spectral range and resolution compensate for those limitations.

4.5. Burnt area delineation based on Sentinel-1

The information provided by the MTC images was adequate to automatically delineate the extent of the burnt area. Similar results were obtained by Donezar et al. (2017). This methodology, developed in a steep terrain AOI, and tested in an area with more sparse vegetation than the area studied in 2017, showed the importance of having images acquired in ascending and descending modes to decrease the influence of the terrain in the results. These results are similar to the findings by Ferretti et al. (2017b). The integration of automatic classification of MTC images to detect burnt areas and the use of optical imagery or other ancillary data to refine the fire delineation by photo-interpretation would be suitable to obtain accurate thematic layers.

Acknowledgements

References

Broglia, M., Corbane, C., Carrion, D., Lemoine, G., and Pesaresi, M. 2010. Validation Protocol for Emergency Response Geo-information Products. JRC59838. *JRC technical reports*. Luxembourg. http://publications.jrc.ec.europa.eu/repository/handle/JRC59838.

Closson, D., Milisavljevic, N. 2017. InSAR Coherence and Intensity Changes Detection. In *Mine Action - The Research Experience of the Royal Military Academy of Belgium*. https://doi.org/10.5772/65779

Cocke, A.E., Fule, P.Z., Crouse, J.E. 2005. Comparison of burn severity assessments using Differenced Normalized Burn Ratio and ground data. *International Journal of Wildland Fire, 14*(2), pp. 189-198. https://doi.org/10.1071/WF04010

CEMS, Copernicus Emergency Management Service, 2017. Early Warning and monitoring. Floods and forest fires. Available at: https://emergency. copernicus.eu/mapping/ems/early-warning-systems-efas-and-effis

CEMS, Copernicus Emergency Management Service, 2018. Copernicus Emergency Management Service - Mapping, Manual of Operational Procedures. Available at: https://emergency.copernicus.eu/ mapping/sites/default/files/files/EMS_Mapping_ Manual_of_Procedures_v1_3_final.pdf

CEMS, Copernicus Emergency Management Service, 2020. Service overview. https://emergency. copernicus.eu/mapping/sites/default/files/files/ CopernicusEMS-Service_Overview_Brochure.pdf

Copernicus Space Component Data Access. Available: https://spacedata.copernicus.eu/

Copernicus Space Component Data Access (ESA). 2020. Contributing Mission. Available at: https:// spacedata.copernicus.eu/web/cscda/data-offer/ mission-groups

Donezar, U., Larrañaga, A., Tamés, A., Sánchez, C., Albizua, L., Ciriza, R., Del Barrio, F. 2017. Applicability of Sentinel-1 and Sentinel-2 Images for the Detection and Delineation of Crisis Information in the Scope of Copernicus EMS Services. *Revista de Teledetección*, *50*, 49-57. https://doi.org/10.4995/raet.2017.8896

Donezar, U., De Blas, T., Larrañaga, A., Ros, F., Albizua, L., Steel, A., Broglia, M. 2019. Applicability of the MultiTemporal Coherence Approach to Sentinel-1 for the Detection and Delineation of Burnt Areas in the Context of the Copernicus Emergency Management Service. *Remote Sens., 11*(22), 2607. https://doi.org/10.3390/rs11222607

ESA, a. European Space Agency. N.d. a. Sentinel Online. Technical Guides. Available at: https://sentinel.esa. int/web/sentinel/technical-guides/sentinel-1-sar/ products-algorithms/level-1-algorithms/products

ESA, b. European Space Agency. N.d. b. Sentinel Online. Technical Guides. Available at: https:// sentinel.esa.int/web/sentinel/user-guides/sentinel-1-sar/resolutions/level-1-single-look-complex

ESA, c. European Space Agency. N.d. c. Sentinel Online. Technical Guides. Available at: https://earth. esa.int/web/sentinel/user-guides/sentinel-2-msi/ product-types

ESA, d. European Space Agency (ESA). N.d. d Step (Science toolbox exploitation platform). Sen2Cor. Available at: https://step.esa.int/main/third-party-plugins-2/sen2cor

ESA, e. European Space Agency (ESA). N.d. e. ERS Radar Courses. Available at: https://earth.esa.int/ web/guest/missions/esa-operational-eo-missions/ ers/instruments/sar/applications/radar-courses/ content-2/-/asset_publisher/qIBc6NYRXfnG/ content/radar-course-2-parameters-affecting-radar-backscatter

Ferretti, A., Monti-Guarnieri, A., Prati, C., Rocca, F. 2017a. Part A - Interferometric SAR image processing and interpretation. In InSAR Principles: Guidelines for SAR Interferometry Processing and Interpretation; Fletcher, K., Ed.; ESA Publications: Noordwijk, The Netherlands.

Ferretti, A., Monti Guarnieri, A., Prati, C., Rocca, F. 2017b. Part B - InSAR processing: A practical approach. In InSAR Principles: Guidelines for SAR interferometry processing and interpretation; Fletcher, K., Ed.; ESA Publications: Noordwijk, The Netherlands.

Fornacca, D., Ren, G.P., Xiao, W. 2018. Evaluating the best spectral indices for the detection of burn scars at several post-fire dates in a mountainous region of Northwest Yunnan, China. *Remote Sensing, 10*(8), 1196. https://doi.org/10.3390/rs10081196

Henry, J.B., Chastanet, P., Fellah, K., Desnos, Y.L. 2006. Envisat Multi-Polarized ASAR Data for Flood Mapping. *International Journal of Remote Sensing, 27*(10), 1921-1929. https://doi.org/10.1080/01431160500486724

Jo, M., Batuhan, O., Zhang, B., Wdowinski, S. 2018. Flood extent mapping using dual-polarimetric Sentinel-1 synthetic aperture radar imagery. In: *ISPRS - International Archives of the Photogrammetry, Remote Sensing and Spatial Information Sciences*. XLII-3, pp. 711-713. https://doi.org/10.5194/isprs-archives-XLII-3-711-2018

Lencinas, J.D., Siebert, A. 2009. Relevamiento de bosques con información satelital: Resolución espacial y escala. *Quebracho, 17*(1,2), 101-105.

Lu, Z., Zhang, L. 2014. Frontiers of Radar Remote Sensing. *Photogrammetric Engineering & Remote Sensing*, *80*, 5-13.

Pekel J.F., Cottam A., Gorelick N., Belward, A.S. 2016. High-resolution mapping of global surface water and its long-term changes. *Nature, 540*, 418-422. https://doi.org/10.1038/nature20584

Priego, A., Bocco, G., Mendoza, M., Garrido, A. 2010. *Propuesta para la generación semiautomatizada de unidades de paisaje: Serie Planeación territorial. Procedimiento para el levantamiento y cartografía de las unidades superiores de los paisajes a escalas 1:50,000 y 1:250,000*, pp. 33-52., UNAM, Mexico.

Shen, X., Wang, D., Mao, K., Anagnostou, E., Hong, Y. 2019. Inundation Extent Mapping by Synthetic Aperture Radar: A Review. *Remote Sensing, 11*, 879. https://doi.org/10.3390/rs11070879

Tanase, M.A., De la Riva, J., Santoro, M., Perez-Cabello, F., and Kasischke, E.S. 2011. Sensitivity of SAR data to post-fire forest regrowth in Mediterranean and boreal forests. *Remote Sensing of Environment, 115*, 2075-2085. https://doi.org/10.1016/j.rse.2011.04.009

Textron systems. Available at https://www.textronsystems.com/products/feature-analyst

U.S. Geological Survey (USGS). N.d. EROS Data Center. SRTM 1 Arc-Second global. Available at: https://www.usgs.gov/centers/eros/science/usgs-eros-archive-digital-elevation-shuttle-radar-topography-mission-srtm-1-arc?qt-science_center_objects=0#qt-science_center_objects